REWETTING OF AN INFINITE SLAB WITH BOUNDARY HEAT FLUX

Authors: Satapathy A. K.; Kar P. K.
aksatapathy2003@rediffmail.com

Source: Numerical Heat Transfer Part A: Applications, Volume 37, Number 1, 1 January 2000 , pp. 87-99(13)

Publisher: Taylor and Francis Ltd

Abstract:
This paper deals with a numerical solution of the two-dimensional quasi-static conduction equation, governing conduction controlled rewetting of an infinitely long slab with one side flooded and the other side subjected to a constant heat flux. The solution gives the quench front temperature as a function of various model parameters such as Peclet number, Biot number, and dimensionless boundary heat flux. Also, the critical boundary heat flux is obtained by setting the Peclet number equal to zero, which gives the minimum heat flux required to prevent the hot surface being rewetted.

REWETTING OF AN INFINITE SLAB WITH BOUNDARY HEAT FLUX

A. K. Satapathy and P. K. Kar
Department of Mechanical Engineering, Regional Engineering College, Rourkela-769 008, Orissa, India

This paper deals with a numerical solution of the two-dimensional quasi-static conduction equation, governing conduction controlled rewetting of an infinitely long slab with one side flooded and the other side subjected to a constant heat flux. The solution gives the quench front temperature as a function of various model parameters such as Péclet number, Biot number, and dimensionless boundary heat flux. Also, the critical boundary heat flux is obtained by setting the Péclet number equal to zero, which gives the minimum heat flux required to prevent the hot surface being rewetted.

INTRODUCTION

The process of quenching of hot surfaces is of practical importance in nuclear and metallurgical industries. For instance, after a hypothetical loss-of-coolant accident (LOCA) in water-cooled reactors, the temperature of the clad surface of the fuel elements would increase drastically because the stored energy in the fuel and the decay heat cannot be removed adequately by the surrounding steam. In order to prevent the fuel from reaching a metallurgically prohibitive temperature, an emergency core cooling system is activated to reflood the core. The time delay in reestablishing effective cooling may result in a cladding temperature rise, significantly above the saturation temperature. If the cladding temperature rises above the rewetting temperature, a stable vapor blanket will prevent the immediate return to liquid-solid contact. Rewetting is the reestablishment of liquid contact with a hot cladding surface and, thereby, bringing it to an acceptable temperature. Also, the quenching phenomenon is of considerable practical interest in many other applications, such as steam generators, evaporators, cryogenic systems, and metallurgical processing.

The cooling process during quenching is characterized by the formation of a wet patch on the hot surface, which eventually develops into a steadily moving quench front. As the quench front progresses along the hot solid, the upstream end of the solid is cooled by convection to the contacting liquid, while its downstream end is cooled by heat transfer to a mixture of vapor and entrained liquid droplets, called precursory cooling. In a realistic nuclear reactor situation the decay heat is generated by fission. Consequently, the cladding is heated due to heat transfer from the fuel. Thus the cladding can be modeled as a heated slab with a specified heat flux on one side and without any heat source.

NOMENCLATURE

B	Biot number	α	stretching parameter
C	specific heat	δ	thickness of the slab
h	heat transfer coefficient	θ	dimensionless temperature
k	thermal conductivity	ξ, η	coordinates after infinite-finite
L	length of the slab		transformation
Pe	Péclet number	ρ	density
q	heat flux		
Q	dimensionless heat flux		
t	time	**Subscripts**	
T	temperature		
u	quench front velocity	s	saturation
x, y	physical coordinates	w	wall condition
$\bar{x}, \bar{y}$	coordinates in quasi-steady state	0	quench front
X, Y	dimensionless coordinates in	1	wet region
	quasi-steady state	2	dry region

Estimation of rewetting (quench front) temperature is essential in predicting the rate at which the reentering coolant quenches the core. The rewetting model for a two-dimensional two-region heat transfer with a step change in heat transfer coefficient at the quench front has been solved for a single slab [1–6] or for a composite slab [7]. In the single slab model the unwetted side is considered to be adiabatic, whereas in the case of a composite slab a three-layer composite is considered to simulate the fuel and the cladding separated by a gas-filled gap between them. The solution methods employed are either separation of variables or the Wiener-Hopf technique. A rewetting model for a vertical surface with uniform heat flux and precursory cooling has been solved by an approximate integral method [8]. The transient one-dimensional rewetting equation with uniform heat flux has been solved numerically as well as analytically by Chan and Zhang [9]. A time dependent plate temperature at far downstream of the quench front has been suggested to overcome the incompatibility matching condition in their analytical solution. Ferng et al. [10] considered the conjugate heat transfer model in an axisymmetric geometry. The governing equations in the solid and fluid regions have been solved simultaneously by the finite difference method to obtain the complete boiling curve. The temperature dependent physical properties used in their solution have been calculated from the boiling curve.

In the present study the rewetting model due to Yao [8] has been adopted. The physical model consists of an infinitely extended vertical slab with one side flooded and the other side subjected to uniform heat flux to simulate the decay heating of the fissile material. The model assumes constant but different heat transfer coefficients for the wet and dry regions on the flooded side. The two-dimensional quasi-static conduction equation governing conduction controlled rewetting of the infinite slab has been solved by the finite difference method. A numerical model is proposed to solve the class of problems in conduction-controlled rewetting so that it can be extended to problems in various other

geometries. The model is validated by comparing the results with known closed form solutions.

The numerical solution of the rewetting problem encounters two major difficulties: first, the infinite domain of the slab and the prescription of the temperature at the boundary at infinity. This problem is alleviated by transforming the infinite physical domain to a finite computational domain by a suitable mapping function. The value of the stretching parameter associated with the transformation has been found by minimizing the overall heat balance. Second, a jump in the boundary condition at the quench front yields a singularity as observed by Blair [1] and Olek [3] in their analytical solutions. In the context of the present numerical treatment, the presence of this singularity may give rise to accuracy problems. This has been overcome by imposing the continuity matching condition for both the temperature and the heat flux at the quench front as described in the text.

MATHEMATICAL MODEL

The two-dimensional transient heat conduction equation for the slab is

$$k\left(\frac{\partial^2 T}{\partial x^2}+\frac{\partial^2 T}{\partial y^2}\right)=\rho C\frac{\partial T}{\partial t} \qquad 0<x<\delta \qquad 0<y<L \qquad L\to\infty \tag{1}$$

where L is the length of the slab and δ is the thickness of the slab. The density, specific heat, and thermal conductivity of the slab material are ρ, C, and k, respectively. The origin of the coordinate frame is at the left bottom corner of the slab. To convert this transient equation into quasi-steady state, the following transformation is used:

$$\bar{x}=x \qquad \bar{y}=y-ut$$

where u is the constant quench front velocity and $\bar{x}$ and $\bar{y}$ are normal and axial coordinates, respectively (Figure 1). Thus the transformed heat conduction equation in a coordinate system moving with the quench front at this velocity is

$$\frac{\partial^2 T}{\partial \bar{x}^2}+\frac{\partial^2 T}{\partial \bar{y}^2}+\frac{\rho C u}{k}\frac{\partial T}{\partial \bar{y}}=0 \qquad 0<\bar{x}<\delta \qquad -\infty<\bar{y}<\infty \tag{2}$$

In conduction controlled rewetting analysis, it is believed that conduction of heat along the slab from the dry region to the wet region is the dominant mechanism of heat removal ahead of the quench front, which results in a lowering of the surface temperature immediately downstream of the quench front and causes the quench front to progress further. Since only axial conduction is considered, the effect of coolant mass flux, coolant inlet subcooling and its pressure gradient, etc., are not accounted for explicitly, but only implicitly in terms of wet region heat transfer coefficient, which is incorporated in the boundary condition. In the present analysis the heat transfer coefficient h_1 is assumed to be constant

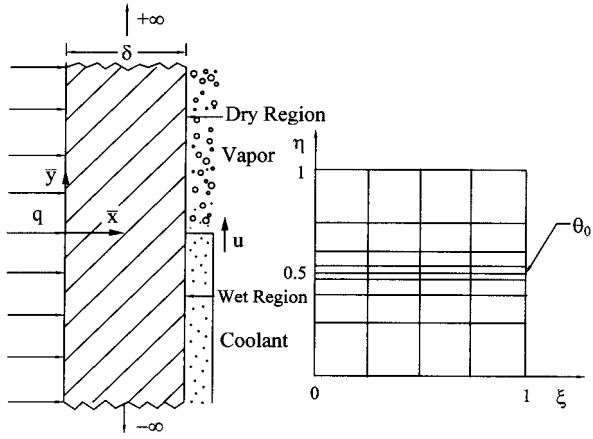

Figure 1. Physical and computational domain of an infinite slab.

over the entire wet region. The coolant temperature is taken to be equal to its saturation temperature T_s. On the dry side of the slab the wall is cooled by the surrounding gas. This cooling effect is very small as compared to that of the wet region and is usually neglected in many rewetting models. However, this small cooling mechanism is very important in studying the rewetting of a fuel rod with an internal heat source and cannot be neglected [8]. The heat transfer coefficient accounting for both convective and radiative cooling effects on the dry side is assumed equal to h_2, a constant, which is smaller than h_1. The temperature of the surrounding gas is assumed equal to T_w, which can be interpreted as the steady state temperature of the hot surface prior to the occurrence of the loss-of-coolant accident. Although the existence of boundary heat flux may cause an unsteady value of T_w, the net vapor generated at the liquid-vapor interface may partially offset any increase in the gas temperature. Hence the value of T_w may be assumed to be constant, as suggested by Yao [8]. Equation (2) can be expressed in the following dimensionless form:

$$\frac{\partial^2\theta}{\partial X^2} + \frac{\partial^2\theta}{\partial Y^2} + \mathrm{Pe}\frac{\partial\theta}{\partial Y} = 0 \qquad 0 < X < 1 \qquad -\infty < Y < \infty \tag{3}$$

The associated boundary conditions are

$$\begin{aligned} &\frac{\partial\theta}{\partial X} + Q = 0 && X = 0 && -\infty < Y < \infty \\ &\frac{\partial\theta}{\partial X} + B_1\theta = 0 && X = 1 && Y < 0 \\ &\frac{\partial\theta}{\partial X} + B_2(\theta - 1) = 0 && X = 1 && Y > 0 \end{aligned} \tag{4}$$

The nondimensional variables used above are

$$X = \frac{\bar{x}}{\delta} \qquad Y = \frac{\bar{y}}{\delta} \qquad \theta = \frac{T - T_s}{T_w - T_s} \qquad B_1 = \frac{h_1 \delta}{k} \qquad B_2 = \frac{h_2 \delta}{k}$$
$$\mathrm{Pe} = \frac{\rho C u \delta}{k} \qquad Q = \frac{q\delta}{k(T_w - T_s)} \tag{5}$$

The boundary conditions in Eq. (4) require liquid/gas temperatures and liquid/gas heat transfer coefficients as input parameters, these limitations being inherent in a conduction-controlled rewetting analysis. However, the arbitrariness of the choice of their values can be eliminated if a conjugate heat transfer model [10] is considered. Following Yao [8], it may be envisaged that the temperature field is sufficiently flat in the Y direction at infinity. Consequently, the first and second derivatives of temperature in the Y direction can be neglected far upstream of the quench front (at $Y \to -\infty$) as well as far downstream of the quench front (at $Y \to +\infty$). The above two assumptions are adequate to prescribe the temperature at infinity ($Y \to \pm\infty$). The corresponding boundary conditions then become

$$\theta = \frac{Q}{B_1} + Q(1 - X) \qquad Y \to -\infty$$
$$\theta = 1 + \frac{Q}{B_2} + Q(1 - X) \qquad Y \to +\infty \tag{6}$$

It may be verified that for a condition of no heat flux with adiabatic dry side (by setting $Q/B_2 = 0$ and $Q = 0$), the boundary conditions (Eq. (6)) reduce to that of the conventional two-region model (insulated dry wall and no heat source [3]). The main interest of the present analysis is to solve for the quench front temperature T_0 for given values of wet side Biot number B_1, dry side Biot number B_2, Peclet number Pe, and dimensionless heat flux Q. The nondimensional quench front temperature is defined by

$$\theta_0 = \frac{T_0 - T_s}{T_W - T_s} = \theta(1, 0) \tag{7}$$

The infinite physical domain ($-\infty < Y < +\infty$) is then mapped to a finite computational domain (Figure 1) by the following the infinite-finite transformation:

$$\xi = X \qquad \eta = 0.5(1 + \tanh \alpha Y)$$

where α is the stretching parameter. The rationale of such a transformation is that the analytical boundary conditions at infinity can be used in the finite-difference equations. The conduction equation, Eq. (3), is thus transformed to

$$\frac{\partial}{\partial \xi}\left(\frac{1}{\eta_y}\frac{\partial \theta}{\partial \xi}\right) + \frac{\partial}{\partial \eta}\left(\eta_y \frac{\partial \theta}{\partial \eta} + \mathrm{Pe}\ \theta\right) = 0 \tag{8}$$

where $\eta_y = \partial\eta/\partial Y$. The transformed boundary conditions are

$$\begin{aligned}
&\frac{\partial\theta}{\partial\xi} + Q = 0 && \xi = 0 && 0 < \eta < 1\\
&\frac{\partial\theta}{\partial\xi} + B_2(\theta - 1) = 0 && \xi = 1 && \eta > 0.5\\
&\frac{\partial\theta}{\partial\xi} + B_1\theta = 0 && \xi = 1 && \eta < 0.5\\
&\theta = \frac{Q}{B_1} + Q(1 - \xi) && && \eta = 0\\
&\theta = 1 + \frac{Q}{B_2} + Q(1 - \xi) && && \eta = 1\\
&\theta = \theta_0 && \xi = 1 && \eta = 0.5
\end{aligned} \tag{9}$$

Although Eqs. (8) and (9) have been formulated for quenching by bottom flooding, they are also valid for top flooding.

NUMERICAL SOLUTION

The five-point representation of the elliptic equation, Eq. (8), can be written in the general form

$$A^0_{i,j}\theta_{i,j} = A^1_{i,j}\theta_{i,j+1} + A^2_{i,j}\theta_{i+1,j} + A^3_{i,j}\theta_{i,j-1} + A^4_{i,j}\theta_{i-1,j} + S_{i,j} \tag{10}$$

The coefficients $A_{i,j}$ and the source term $S_{i,j}$ are evaluated by applying the power law scheme [11] which makes use of integrating Eq. (8) over nonuniform control volumes, having a face area of $\Delta\xi\Delta\eta$. This approach remains valid for all grid locations except at the quench front. Since discontinuities in boundary conditions exist at the quench front, the coefficients of the discretized equation at this location have been obtained by an appropriate technique [12]. The $\theta_{i,j}$ at the interface are expanded into Taylor series "forwards" for the dry region and "backwards" for the wet region, dropping terms beyond second order. These equations give $(\partial^2\theta/\partial\eta^2)_{i,j}$ for the dry and wet regions, which when substituted in the nonconservative form of Eq. (8), yields $(\partial\theta/\partial\eta)_{i,j}$ for the dry and wet regions, respectively. Now the expressions for $(\partial\theta/\partial\eta)_{i,j}$ at the interface are put in the following compatibility conditions to determine $A_{i,j}$ and $S_{i,j}$ of the discretized Eq. (10):

$$\left(\frac{\partial\theta}{\partial\eta}\right)^I_{i,j} = \left(\frac{\partial\theta}{\partial\eta}\right)^{II}_{i,j} \qquad (\theta)^I_{i,j} = (\theta)^{II}_{i,j}$$

where superscripts I and II denote dry and wet regions, respectively. Expressions for the coefficients in Eq. (10) are given in the appendix. To solve the system of

algebraic equations thus formed, an alternating direction implicit (ADI) iterative scheme is used. A convergence criterion of 0.01% change in θ at all nodes has been selected to test the convergence of the iterative scheme. All computations have been carried out using a nonuniform grid arrangement with 21×161 nodes. Since steep temperature gradients are encountered near the quench front, a grid structure has been adopted with finer grids near the quench front and progressively coarser grids away from it (Figure 1). Sample calculations were also carried out by doubling the grid size to ensure that the results are independent of the grid system. As evident from the appendix, the coefficients and the source term are independent of temperature, and they do not pose any divergence problem.

Since the main objective of the present study is to estimate the quench front temperature as correctly as possible, it is essential that the temperature field satisfy the heat balance. This is done by integrating Eq. (8) over the entire computational domain, which gives

$$\left(\frac{Q + 0.5B_2}{\alpha}\right)\ln\left(\frac{\eta_{j=n-1}}{\eta_{j=2}}\right) + \int_0^1 \left(\mathrm{Pe}\,\theta + 2\alpha\eta(1-\eta)\left.\frac{\partial\theta}{\partial\eta}\right|_{j=n-1}\right)d\xi$$

$$= B_1\int_{j=2}^{0.5}\frac{\theta}{2\alpha\eta(1-\eta)}d\eta + B_2\int_{0.5}^{j=n-1}\frac{\theta}{2\alpha\eta(1-\eta)}d\eta$$

$$+\int_0^1 \left(\mathrm{Pe}\,\theta + 2\alpha\eta(1-\eta)\left.\frac{\partial\theta}{\partial\eta}\right|_{j=2}\right)d\xi \qquad (11)$$

where n is the number of nodes in the η direction in the grid matrix. The integrals of Eq. (11) have been obtained using Simpson's $1/3$ rule. The absolute difference between the right and left sides of the above equation is first divided by a minimum of the two values and then multiplied by 100 to get the percentage difference.

If the heat balance difference so obtained is assumed to be the objective function, then the stretching parameter associated with mapping can be treated as an independent variable. Thus, starting from an arbitrary base point ($\alpha > 0$), the variable can be moved toward an optimum based on sequential minimization of the objective function. To reduce the number of function evaluations, an optimization technique (Golden Section Search) is used that does not require the derivative of the function. A tolerance limit of 0.01% change of the function value has been selected, below which the search process is terminated.

RESULTS AND DISCUSSION

Experimental investigations on quenching [13] reveal the existence of four distinct heat transfer regimes along the wall, the regimes being demarcated by the characteristic hot surface temperature. These four zones are forced convection of subcooled liquid, nucleate boiling, wet and dry transition boiling, and film boiling. The quench front is observed to exist in the transition zone. The heat transfer coefficient in the transition zone is shown to be 10^5–10^6 W/(m^2 K) and the vapor cooling heat transfer coefficient ahead of the film boiling zone is of the order of 10^2 W/(m^2 K). In the present analysis the values of B_2 are set equal to $10^{-3}B_1$.

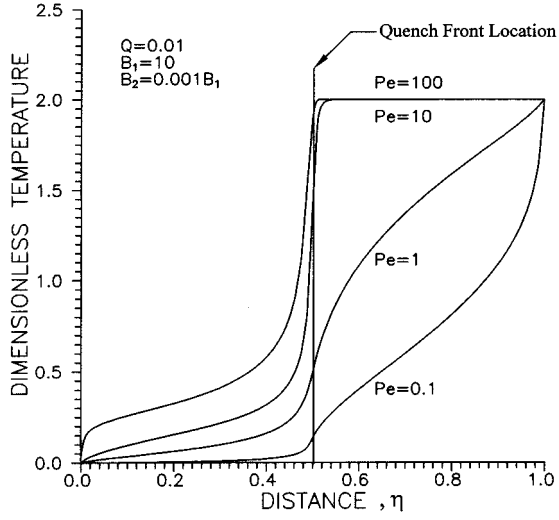

Figure 2. Surface temperature distribution on the coolant side.

The distribution of surface temperatures on the coolant side of the slab are shown in Figure 2 for different Péclet numbers for $Q = 0.01$ and $B_1 = 10.0$. The temperature at $\eta = 1$ (downstream of the quench front) is Q/B_2 higher than the initial wall temperature. Similarly, the temperature at $\eta = 0$ (upstream of the quench front) is Q/B_1 higher than the coolant temperature. At lower values of Péclet number (for Pe = 0.1 and 1.0), a part of the dry region immediately ahead of the quench front has a nondimensional temperature less than 1 and the other part of it is more than 1. This implies that the former part of the dry region will be heated by the vapor instead of being cooled as the temperature of the vapor is assumed to be equal to the initial wall temperature. But in the case of higher Péclet numbers (Pe = 10 and 100), the whole of the dry region is of temperature greater than 1, and it will be cooled by vapor.

Moreover, the quench front temperature as well as the temperature gradient at the quench front are found to increase with increase in Pe (Figure 2). With fixed material properties and dimensions, Pe and Bi number represent the quench front velocity and the heat transfer coefficient respectively. For the prescribed heat flux and Bi numbers the quench front temperature increases with increase in quench front velocity. This may be due to the fact that a higher relative velocity between the slab and the coolant allows less time for sufficient heat transfer to take place, resulting in a higher value of θ_0. The quench front temperature is also found to increase monotonously with increase of Pe. This reflects the fact that for the same rewetting rate, an increasing cladding thermal diffusivity tends to reduce θ_0, whereas the increasing cladding thickness has the opposite effect. The temperature gradient also increases with increase in Pe in the computational domain. This reveals the fact that at higher quench velocities, the axial conduction across the quench front may be significant.

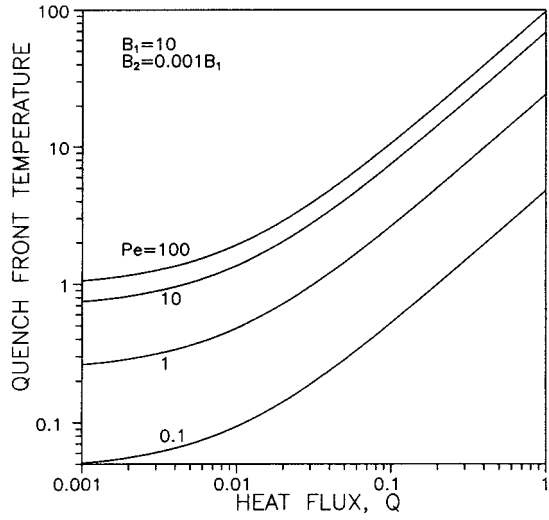

Figure 3. Quench front temperature for various heat flux and Péclet numbers.

Figure 3 shows the dependence of quench front temperature on Pe and dimensionless heat flux. For a fixed Biot number, quench front temperature increases with increase in Pe and Q. Apparently, a higher heat flux causes more heat transfer to the cladding, and hence this would increase θ_0. Also, the quench front temperature decreases with increase in Biot numbers for a given Pe and Q (Figure 4). A higher Biot number results in higher heat transfer coefficient. This enhanced heat transfer coefficient may be the probable cause for the decrease in θ_0 when the Biot number increases. The above trends are in obvious accord with what one would expect on physical grounds. In all cases, θ_0 decreases as Biot number increases, reflecting the fact that a quench front progresses more easily when the heat transfer coefficient to the coolant is increased. On a similar ground, one would conclude that an increasing Q has the opposite effect on the quench front velocity.

Figure 5 shows the dependence of quench front temperature with Biot number and dimensionless heat flux for Pe $= 0$. The physical meaning of Pe $= 0$ is that the quench front stops when Q approaches its critical value. This is the case in which the slab can no longer be wetted. For $Q > Q_{cri}$ the wet front will reverse its direction, and the wetted surface will be dried, which is not a realistic case for a nuclear reactor. Moreover, the magnitude of critical boundary heat flux is directly proportional to the Biot number and the dimensionless quench front temperature. A good agreement of data with those of Yao [8] is also depicted in the figure.

Last, the model is reduced to that of the conventional model (dry insulated wall and no precursory cooling). By setting $Q = 0$ the present model simulates the flooding situation of a hot slab of thickness 2δ, and due to the plane of symmetry, half of its thickness can be analyzed. The present solution has been compared with those of Olek [3], and a good agreement of data is observed in Figure 6. The

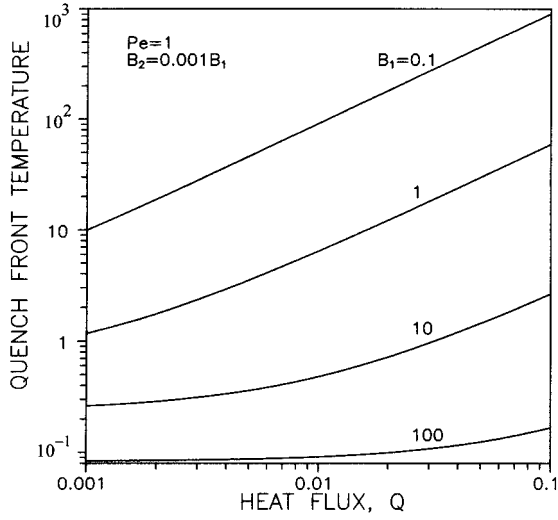

Figure 4. Quench front temperature for various heat flux and Biot numbers.

present solution has also been compared with the steady state solutions of Chan and Zhang [10] in Figure 6. Their solution predicts higher values of θ_0 for large Pe, which may be due to the one-dimensional assumption in their model. As expected, the quench front temperature increases with increase in Pe and with decrease in Biot number.

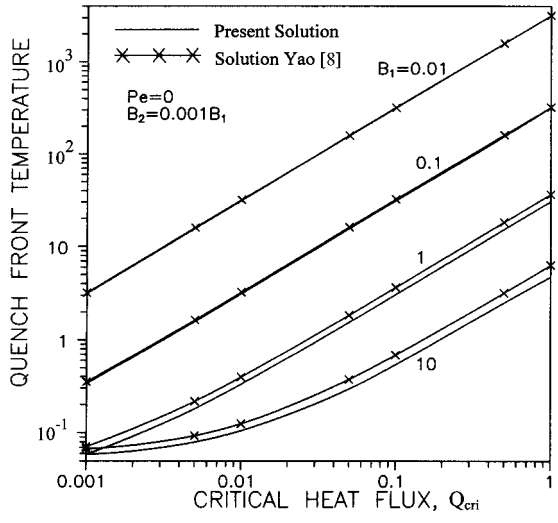

Figure 5. Quench front temperature at critical heat flux.

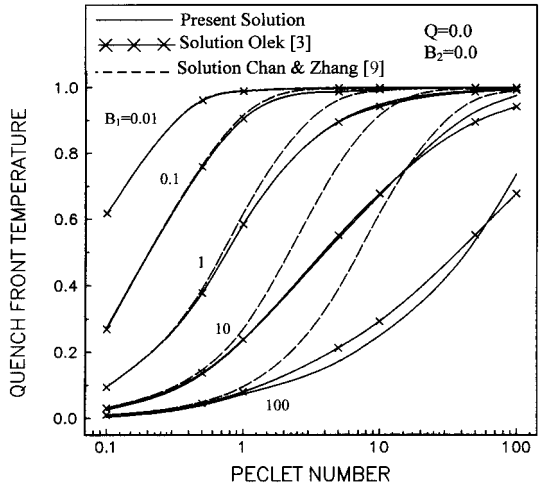

Figure 6. Quench front temperature for various wet side Biot numbers and Péclet numbers without heat generation and vapor cooling.

CONCLUSION

A numerical solution for solving infinite domain problems arising out of rewetting analysis has been suggested. The value of the stretching parameter used for infinite-finite transformation can be obtained by minimizing the heat balance. The results computed with variable mesh size show good agreement with known closed form solutions. In general, quench front temperature is found to increase with increase in Pe and dimensionless heat flux and with decrease in Biot number. It is felt that the present solution procedure, in principle, can be extended to other infinite domain conduction-controlled rewetting problems in various other geometries.

REFERENCES

1. J. B. Blair, An Analytical Solution to a Two-dimensional Model of the Rewetting of a Hot Dry Rod, *Nucl. Eng. Design*, vol. 32, pp. 159–170, 1975.
2. R. E. Caflish and J. B. Keller, Quench Front Propagation, *Nucl. Eng. Design*, vol. 65, pp. 97–102, 1981.
3. S. Olek, On the Two-Region Rewetting Model with a Step Change in the Heat Transfer Coefficient, *Nucl. Eng. Design*, vol. 108, pp. 315–322, 1988.
4. H. Levine, On a Mixed Boundary Value Problem of Diffusion Type, *Appl. Sci. Res.*, vol. 39, pp. 261–276, 1982.
5. C. L. Tien and L. S. Yao, Analysis of Conduction Controlled Rewetting of a Vertical Surface, *J. Heat Transfer, Trans. ASME, Ser. C*, vol. 97, pp. 161–165, 1975.

6. F. Castiglia, E. Olivery, S. Taibi, and G. Vella, Exact Solution to the Two-Dimensional Approach of the Rewetting by a Falling Film, *8th Int. Heat Transfer Conf., San Francisco, California*, pp. 1983–1986, August 1986.
7. S. Olek, Quenching of a Composite Slab, *Int. Commun. Heat Mass Transfer*, vol. 21, pp. 333–344, 1994.
8. L. S. Yao, Rewetting of a Vertical Surface with Internal Heat Generation, *AIChE Symp. Ser.*, vol. 73, pp. 46–50, 1977.
9. S. H. Chan and W. Zhang, Rewetting Theory and the Dryout Heat Flux of Smooth and Grooved Plates with a Uniform Heating, *J. Heat Transfer, Trans. ASME*, vol. 116, pp. 173–179, 1994.
10. Y. M. Ferng, C. C. Chieng, and C. Pan, Predictions of Rewetting Process for a Nuclear Fuel Rod Using First-Principles Equations, *Nucl. Eng. Design*, vol. 126, pp. 189–205, 1991.
11. S. V. Patankar, *Numerical Heat Transfer and Fluid Flow*, 96 pp., Hemisphere, Washington, D.C., 1980.
12. B. Carnahan, H. A. Luther, and J. O. Wilkes, *Applied Numerical Methods*, 462 pp., John Wiley, New York, 1969.
13. Y. Barnea, E. Elias, and I. Shai, Flow and Heat Transfer Regimes During Quenching of Hot Surfaces, *Int. J. Heat Mass Transfer*, vol. 37, pp. 1441–1453, 1994.

APPENDIX: COEFFICIENTS OF FINITE DIFFERENCE EQUATIONS

The internal and boundary nodes (except at the quench front) are

$$A^1_{i,j} = \frac{\eta_y^+}{h_2}\left\| 0 \quad \left(1 - \frac{0.1\mathrm{Pe}\, h_2}{\eta_y^+}\right)^5 \right\| + \mathrm{Pe} \qquad A^2_{i,j} = f_1\left(\frac{2I(\eta)}{h_1}\right)$$

$$A^3_{i,j} = \frac{\eta_y^-}{h_4}\left\| 0 \quad \left(1 - \frac{0.1\mathrm{Pe}\, h_4}{\eta_y^-}\right)^5 \right\| \qquad A^4_{i,j} = f_2\left(\frac{2I(\eta)}{h_3}\right)$$

$$A^0_{i,j} = \sum_{k=1}^{4} A^k_{i,j} + 2f_3 I(\eta) \qquad S_{i,j} = 2f_4 I(\eta)$$

Parallel line enclosures denote the larger between the two values.

For internal nodes,

$$f_1 = f_2 = 1/(h_1 + h_3) \qquad f_3 = f_4 = 0$$

For boundary nodes,

$(\xi = 0)$	$f_1 = 1/h_1$	$f_2 = f_3 = 0$	$f_4 = Q/h_1$
$(\xi = 1, \eta > 0.5)$	$f_1 = 0$	$f_2 = 1/h_3$	$f_3 = f_4 = B_2/h_3$
$(\xi = 1, \eta < 0.5)$	$f_1 = f_4 = 0$	$f_2 = 1/h_3$	$f_3 = B_1/h_3$

The quench front node ($\xi = 1,\ \eta = 0.5$):

$$A^1_{i,j} = \frac{1}{2}\left(\mathrm{Pe} + \frac{\alpha}{h_2}\right)\left(\mathrm{Pe} + \frac{\alpha}{h_4}\right) \qquad A^2_{i,j} = 0 \qquad A^3_{i,j} = \frac{1}{2}\left(\frac{\alpha}{h_4}\right)^2$$

$$A^4_{i,j} = \frac{2}{h_3^2}\left(1 + \frac{h_2}{h_4} + \frac{\mathrm{Pe}\ h_2}{\alpha}\right) \qquad A^0_{i,j} = \sum_{k=1}^{4} A^k_{i,j} + \frac{2B_1}{h_3} + \frac{2B_2}{h_3}\left(\frac{h_2}{h_4} + \frac{\mathrm{Pe}\ h_2}{\alpha}\right)$$

$$S_{i,j} = \frac{2B_2}{h_3}\left(\frac{h_2}{h_4} + \frac{\mathrm{Pe}\ h_2}{\alpha}\right)$$

where

$$I(\eta) = \frac{1}{2\alpha}\ln\left(\frac{\eta^+}{\eta^-}\frac{1-\eta^-}{1-\eta^+}\right) \qquad \eta_y = 2\alpha\eta(1-\eta)$$

$$h_1 = \xi_{i+1} - \xi_i \qquad h_2 = \eta_{j+1} - \eta_j \qquad h_3 = \xi_i - \xi_{i-1} \qquad h_4 = \eta_j - \eta_{j-1}$$

Superscript plus and minus denote $i, j + 1/2$ and $i, j - 1/2$ locations.